Journal of Solid State Chemistry 272 (2019) 38–46

Contents lists available at ScienceDirect

Journal of Solid State Chemistry

journal homepage: www.elsevier.com/locate/jssc

# The combined effect of $CaF_2$ and graphite two-layer coatings on improving the electrochemical performance of Li-rich layer oxide material

Min Li[a,b], Huiya Wang[a,b], Limin Zhao[a,b], Fang Zhang[b,*], Dannong He[a,b,**]

[a] School of Material Science and Engineering, Shanghai Jiao Tong University, No.800 Dongchuan Road, Shanghai 200240, PR China
[b] National Engineering Research Center for Nanotechnology, No.28 East Jiangchuan Road, Shanghai 200241, PR China

ARTICLE INFO

*Keywords:*
Lithium-rich
$CaF_2$ and Graphite two-coating
Cathode material
Capacity decay

ABSTRACT

Although Lithium-rich layered oxide material has a higher discharge specific capacity than conventional commercial cathode materials, the voltage/capacity decay, which are observed during cycle, limit its wider applicability. In this work, $CaF_2$ and Graphite two-layer coatings is first employed to settle these problems. $CaF_2$, acting as the inner coating layer, has excellent Lithium-ion migration velocity and good stability in acidic electrolytes. Graphite, acting as the outer coating layer, can decrease the interfacial resistance of lithium insertion/extraction and enhance the stability of inner material. Attributing to the combined effect of $CaF_2$ and Graphite two-layer coatings, the electrochemical performance of $CaF_2$ and Graphite two-layer coatings lithium-rich layered oxide material (named as LLMO-I) has been improved notably. In details, compared with referential sample, the discharge specific capacity of LLMO-I reaches 215.2 mA h $g^{-1}$ at the 0.5 C and 90% of discharge specific capacity retention after 150 cycles. When the charge/discharge rate reaches 5 C, its specific discharge capacity also has 133.6 mA h $g^{-1}$. Furthermore, the results of electrochemical impedance spectroscopy(EIS) also imply that LLMO-I has the least electrode resistance in all samples because of the combined effect of $CaF_2$ and Graphite two-layer coatings. To sum up, The $CaF_2$ and Graphite two-layers coatings would be a promising method, which could further prompt the commercialization of Lithium-rich layered oxide materials.

## 1. Introduction

When we come to the problem of resource shortage, Lithium-ion battery always occurs in our mind. Over the last few decades, in order to prompt the application of battery in our life, all kinds of materials have been researched by people. Cathode materials, acting as a one of most important part in Lithium-ion battery, determine the discharge specific capacity of Lithium-ion batteries to some extent [1–5]. Lithium-rich layered oxide material, which has a higher discharge specific capacity than $LiFePO_4$ and Nickel cobalt manganese ternary material(NCM) when it is conducted in the 2.0–4.8 voltage range [6–9], has attracted more and more researchers turn their work to this field [10].

However, continuous capacity fade, which owns to the deterioration and degradation of active material surface, has been found during the cycling [11–14]. In order to settle this issue, many methods have been employed. Among these ways, surface coating with various inert compounds that are used to protect the active material from the corrode of electrolytes is a feasible method [15–19]. Furthermore, the choice of inert compound, which acting as protective layer, is also important for improving the cycle performance of Lithium-rich layered oxide material [20]. Liu et al. [15] reported the effect of $CaF_2$-coating on Lithium-rich layered oxide material. They found that $CaF_2$-coating can improve the cycling performance of lithium-rich layered oxide material. It exhibited the discharge specific capacity of 141.5 mA h $g^{-1}$ at 3C. However, they neglected the low electronic conductivity of $CaF_2$, which can increase the interfacial resistance for lithium insertion/extraction. Besides, the reason why lithium-rich layered oxide material presents the weak rate capacity is also rare researched in previous work.

In this work, aim to avoid the weakness of Lithium-rich layered oxide material, such as the severe discharge specific capacity decay and poor rate performance, the combined effect of $CaF_2$ and Graphite two-layer coatings has been researched. These results show that LLMO-I exhibit the best performance in all samples.

## 2. Experimental

### 2.1. Preparation of materials

LLMO-I was prepared through the coprecipitation method. The detail processes are presented in Scheme 1. Firstly, the manganese

* Corresponding author.
** Corresponding author at: School of Material Science and Engineering, Shanghai Jiao Tong University, No.800 Dongchuan Road, Shanghai 200240, PR China.
*E-mail addresses:* fangzhang@alumni.sjtu.edu.cn (F. Zhang), hdn_nercn@163.com (D. He).

https://doi.org/10.1016/j.jssc.2019.01.022
Received 20 October 2018; Received in revised form 17 January 2019; Accepted 27 January 2019
Available online 28 January 2019
0022-4596/ 

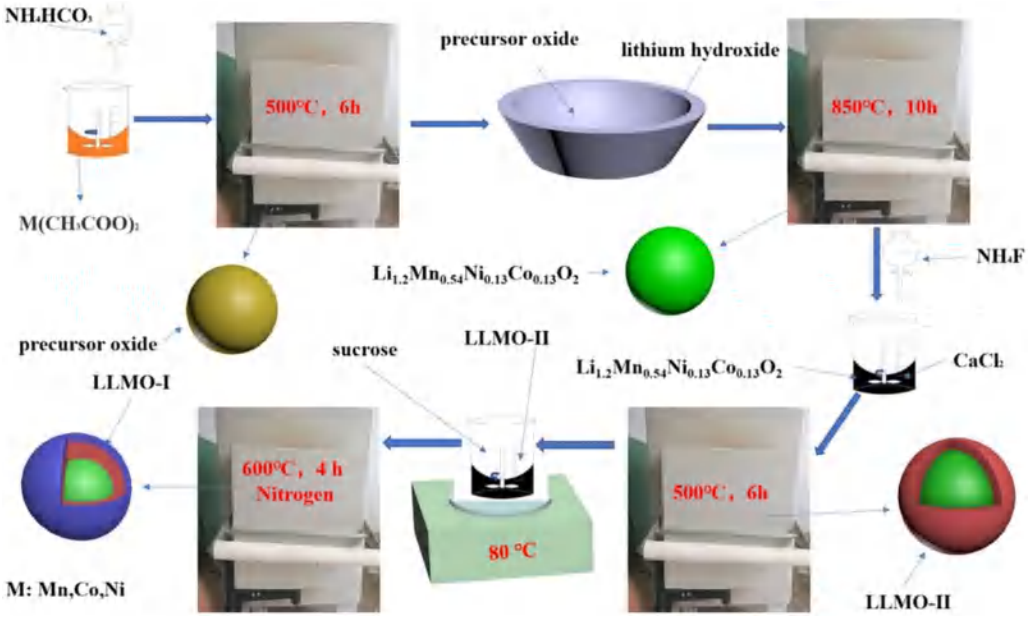


**Scheme 1.** Schematic illustration of the formation process of LLMO-I.

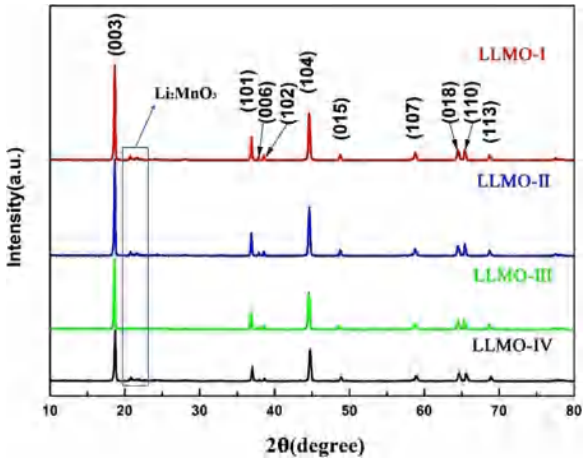


**Fig. 1.** X-ray diffraction patterns of LLMO-I, LLMO-II, LLMO-III, LLMO-IV.

acetate, nickel acetate and cobalt acetate were dissolved in the deionized water in the mole ratio of 54:13:13. Then a certain amount of ammonium bicarbonate solution was instilled into above solution slowly and stirred another 2 h. Afterwards, the obtained solution was filtered, washed and then the precipitate was moved into vacuum drying oven to dry. Finally, the obtained $Ni_{0.13}Co_{0.13}Mn_{0.54}(CO_3)_{0.8}$ was calcined twice to obtain $Li(Li_{0.2}Mn_{0.54}Co_{01.3}Ni_{0.13})O_2$. The detail temperature system can be seen in my previous work [21].

In order to obtain the LLMO-I, the obtained $Li(Li_{0.2}Mn_{0.54}Co_{01.3}Ni_{0.13})O_2$ was dispersed into the solution of calcium chloride firstly, and then a certain amount of ammonium fluoride solution(the mass ratio of $CaF_2$ and $Li(Li_{0.2}Mn_{0.54}Co_{01.3}Ni_{0.13})O_2$ in the percent of 5%) was slowly added into above solution and stirred for 2 h. Afterwards, filtrating and washing were conducted to obtain the mixed powders and then calcined at 500 °C for 6 h. Afterwards, the obtained powder was decentralized into the aqueous sucrose solution and dried at 80 °C under the magnetic stirring. Finally, the above powders were move into tube furnace and calcined at 600 °C for 4 h. All the heat treatments were performed under pure nitrogen atmosphere. The sample of $CaF_2$-coating $Li(Li_{0.2}Mn_{0.54}Co_{01.3}Ni_{0.13})O_2$(named as LLMO-II), Graphite-coating $Li(Li_{0.2}Mn_{0.54}Co_{01.3}Ni_{0.13})O_2$ (named as LLMO-III) and $Li(Li_{0.2}Mn_{0.54}Co_{01.3}Ni_{0.13})O_2$ (named as LLMO-IV) were prepared through the same process.

### 2.2. Materials characterizations and electrochemical measurements

All samples were analyzed through the X-ray diffraction (XRD), Scanning electron microscopy (SEM), transmission electron microscopy (TEM), High resolution transmission electron microscopy (HRTEM) and Energy dispersive X-ray spectrometer (EDS) for getting the information of materials characterizations.

CR2032 coin cells were made up with the Lithium foil, separator, electrolyte (the electrolyte used in the coin cells is high voltage electrolyte, which made in CAPCHEM) and cathode plate. The cathode plate was consisted of 10 mg acetylene black, 10 mg polyvinylidene fluoride (PVDF), 80 mg synthesized active material and 50 ml N-methyl pyrrolidinone (NMP). The stirring time is 4 h. The charge/discharge tests of all samples were conducted at 0.2 C, 0.5 C, 1 C, 2 C, 5 C. The coin cells were scanned on theCHI660B for obtaining the data of cyclic voltammetry and electrochemical impedance spectroscopy.

## 3. Results and discussion

Based on the XRD results of all samples, which present in Fig. 1, some important information about crystal structure can be obtained. Initially, all samples have the same diffraction maximum, which accommodates to the α-$NaFeO_2$ crystal structure well [22]. Besides,the superlattice peaks can be found between 20° and 25°, which are the characteristics of $Li_2MnO_3$-type structure [23]. Additionally, the splitting between (006)/(012) and (018)/(110) can be easily found, which implies all samples have a good layered structure [24]. Moreover, no other diffraction maximum can be found. This indicates $CaF_2$ coating and Graphite coating do not change the crystal structure of Li-rich layered oxide material.

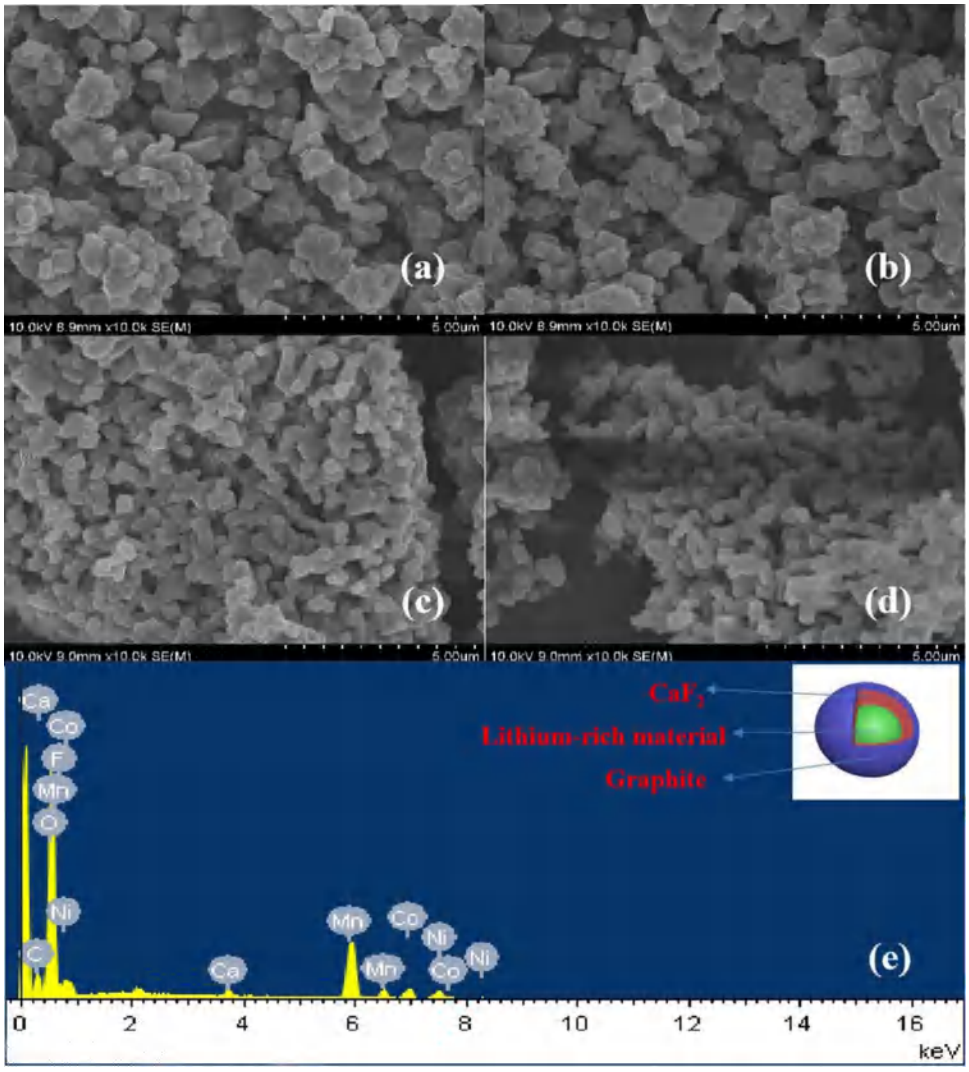


**Fig. 2.** Scanning electron microscope micrograph of (a-d) LLMO-I, LLMO-II, LLMO-III, LLMO-IV, (e) Energy dispersive spectrometer of LLMO-I.

The SEM photographs of all samples are presented in Fig. 2. As shown in Fig. 2a-d, it can be observed that the primary particle morphology of all samples are irregular forms. And the particle size is the range of 500 nm to 2 μm. In order to observe the element distribution on the surface of LLMO-I, EDS was employed. As presented in Fig. 2e, the elements of Ca, F and C are detected on the surface, which mean there are the elements of Ca, F and C on surface of Lithium-rich layered oxide material. Aim to observe the surface microstructure of LLMO-I, the TEM and HRTEM were employed. As shown in Fig. 3a and b, it is notable that the double-layer coatings (Graphite layer and $CaF_2$ layer) was observed on the surface of Lithium-rich layered oxide material. Li-rich layered oxide material and $CaF_2$ layer display well-developed crystallinity (insets of Fig. 3b). Besides, according to the elemental mappings of LLMO -I (Fig. 3c), C, Ca, F, Co, Mn, Ni are observed in LLMO-I.

As shown in Fig. 4, it can be easily observed that all samples have a characteristic of CV curve of Lithium-rich layered oxide material [14,25]. The first anodic peak, which locates at 4.1 V in the initial cycle, on behalf of the redox reaction of $Ni^{2+}/Ni^{4+}$ and $Co^{3+}/Co^{4+}$ [26], and the other anodic peak, which locates at 4.6 V in the initial cycle, on behalf of the redox reaction of $O^{2-}/O$ and $O^{2-}/O^{-}$ [27]. Besides, two reduction peaks, which on behalf of the redox reaction of $Ni^{4+}/Ni^{2+}$, $Co^{4+}/Co^{3+}$ and $Mn^{4+}/Mn^{3+}$, also can be observed at 3.75 V and 3.25 V. The layered $LiMn_2O_3$ has no electrochemical activity. With the activation of $LiMn_2O_3$, its crystal structure gradually changes from layer to spinel, and $Mn^{4+}$ regains its electrochemical activity. As shown in Fig. 4, it is notable that the reduction peak current (correspond to the redox reaction of $Mn^{4+}/Mn^{3+}$ redox couples) of LLMO-I is the least in all samples and its growth rate is also least. It implies that $CaF_2$ and Graphite two-layer coating can restrain the surface phase transition of lithium-rich layered oxide material, which could improve its structural stability and electrochemical performance. The reason of this phenomenon can own to two aspects: firstly, $CaF_2$ and Graphite two-layer coating can protect active material from the erosion of electrolyte; secondly, $F^{-}$, which is offered by $CaF_2$, might diffusion into the Lithium-ion layered oxide material and replace the O-ion at the high temperature, and this transition layer will be a protect layer to inhibit the release of oxygen from Lithium-rich layered oxide material.

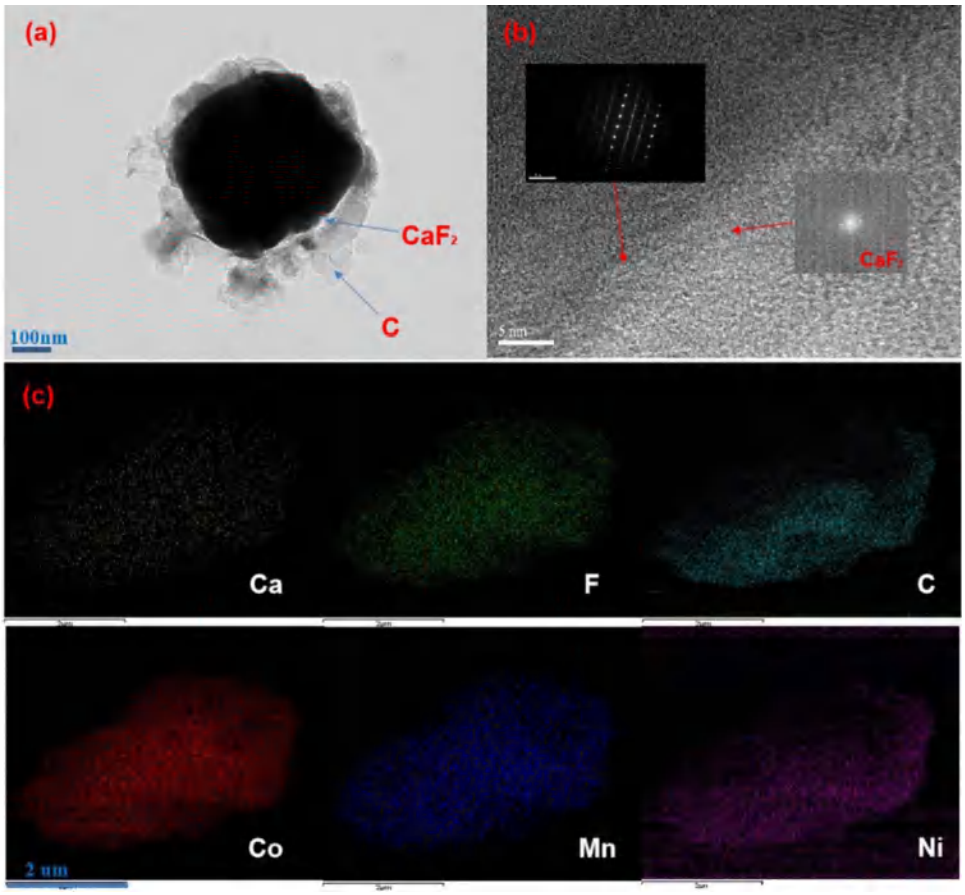


**Fig. 3.** (a) Transmission electron microscope micrograph of LLMO-I; (b) High Resolution transmission electron microscope image of LLMO-I and Selected area electron diffraction of LLMO-I and corresponding Fourier transformation images for CaF2 coating layer; (c) elemental mappings of LLMO-I.

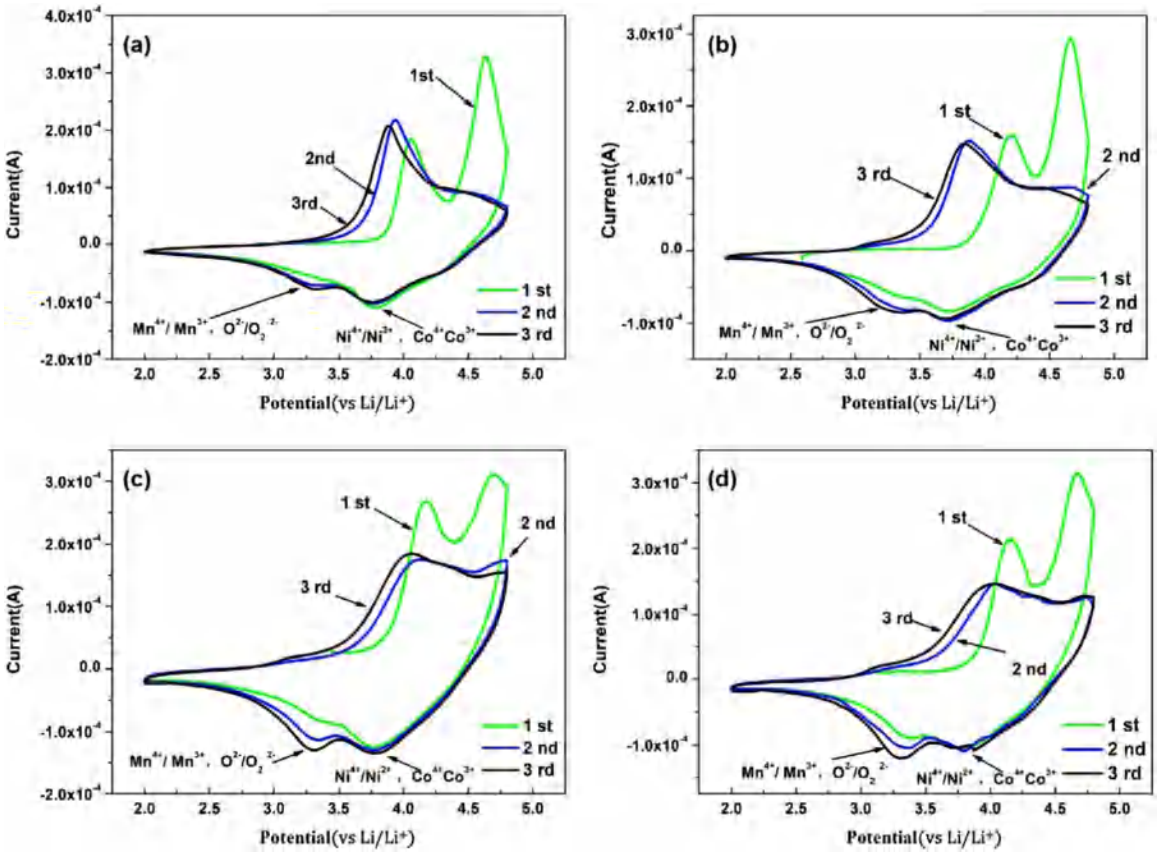


**Fig. 4.** Cyclic Voltammetry curves of (a-d) LLMO-I, LLMO-II, LLMO-III, LLMO-IV.

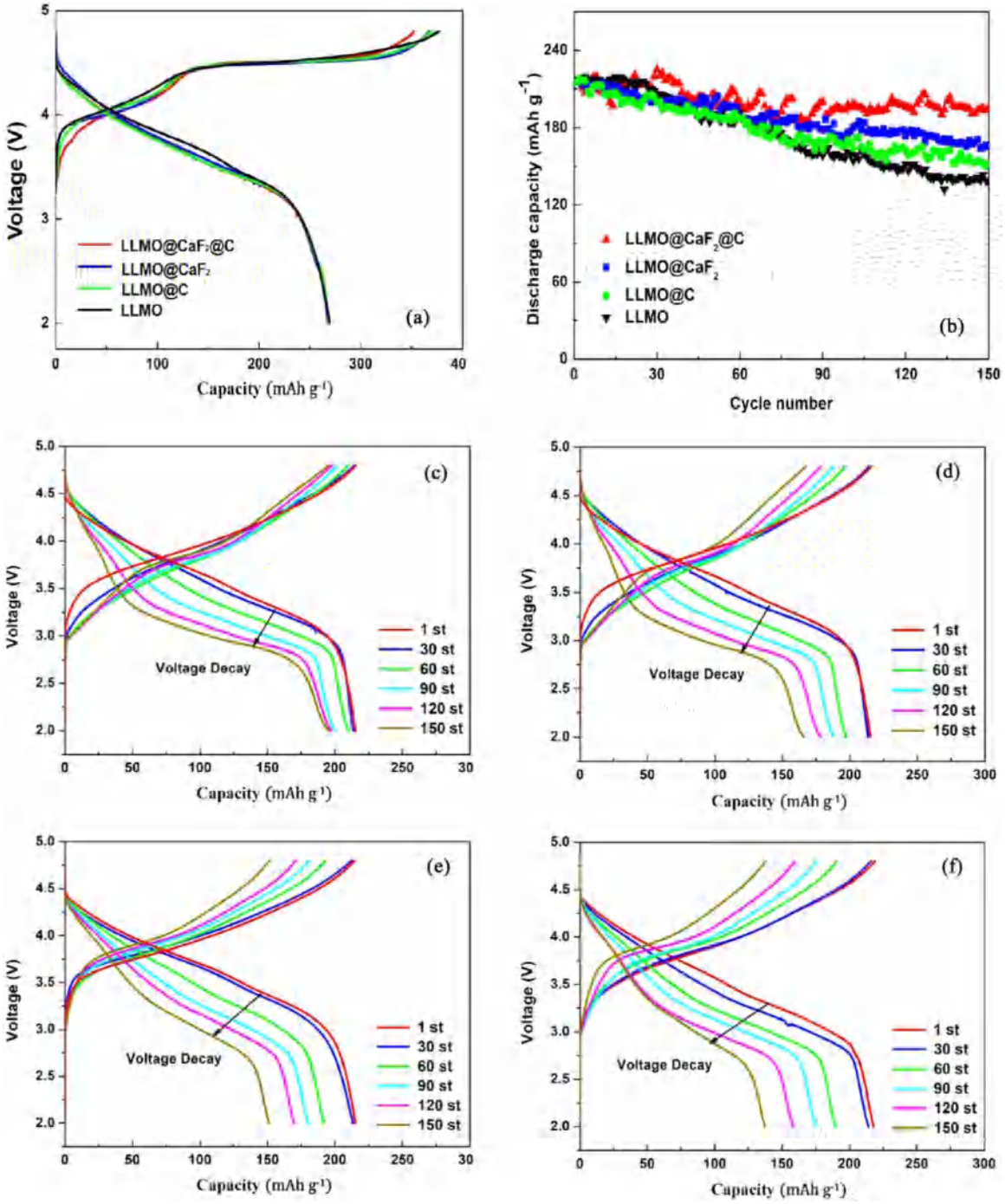


**Fig. 5.** (a) Initial charge–discharge profiles of all samples at 0.1 C, (b) the cycling performance curves of all sample, (c-f) the charge and discharge curves of all samples at 1 st, 30 st, 60 st, 90 st,120 st, 150 st cycle.

**Table 1**
the initial charge-discharge data of LLMO-I, LLMO-II, LLMO-III, LLMO-IV.

| Sample | Initial charge capacity/mA h $g^{-1}$ | Initial discharge capacity/ mA h $g^{-1}$ | Irreversible capacity/ mA h $g^{-1}$ | Initial coulombic efficiency/% |
|---|---|---|---|---|
| LLMO-I | 352.6 | 268.2 | 84.4 | 76.06 |
| LLMO-II | 366.8 | 267.8 | 99.0 | 73.01 |
| LLMO-III | 370.2 | 268.9 | 101.3 | 72.64 |
| LLMO-IV | 377.0 | 269.6 | 107.4 | 71.51 |

**Table 2**
the discharge capacity data LLMO-I, LLMO-II, LLMO-III, LLMO-IV at various rates.

| | Discharge Capacity (mA h $g^{-1}$) | | | | | |
|---|---|---|---|---|---|---|
| | 0.1 C | 0.2 C | 0.5 C | 1 C | 2 C | 5 C |
| LLMO-I | 268.239 | 246.577 | 215.214 | 196.607 | 172.866 | 133.599 |
| LLMO-II | 267.827 | 244.239 | 215.187 | 187.089 | 154.830 | 118.283 |
| LLMO-III | 268.918 | 245.667 | 215.283 | 184.098 | 155.373 | 121.890 |
| LLMO-IV | 269.584 | 248.202 | 217.905 | 178.797 | 146.161 | 107.052 |

Improve the efficiency of initial coulomb efficiency is one of the most important challenge for Lithium-rich layered oxide material. Aim to observe the effect of $CaF_2$ and Graphite two-layer coating on the initial coulomb efficiency of Lithium-rich layered oxide material, all samples were tested at 0.1 C rate between 2.0 and 4.8 V. As presented in Fig. 5a, two charge platforms, which correspond to the characteristic of Lithium-rich layered oxide material type curve, can be found in all samples [28,29]. The first charge platform corresponds to the lithium extraction in lithium layer and the second charge platform above 4.5 V relative to the deinsertion of Lithium-ion from transition metal layer along with the oxygen vacancy occurrence [30,31]. Table 1 is the initial charge/discharge data of all samples. According to Table 1, it is notable that LLMO-I has the least charge specific capacity and the highest initial coulombic efficiency, which can attribute to the $CaF_2$ and Graphite two-layer coating. In order to analyze the effect of $CaF_2$ and Graphite two-layer coatings on cyclic performance of Lithium-rich layered oxide material, all samples are tested at 0.5 C rate between 2.0 and 4.8 V for 150 cycles. As presented in Fig. 5b, LLMO-I displays the

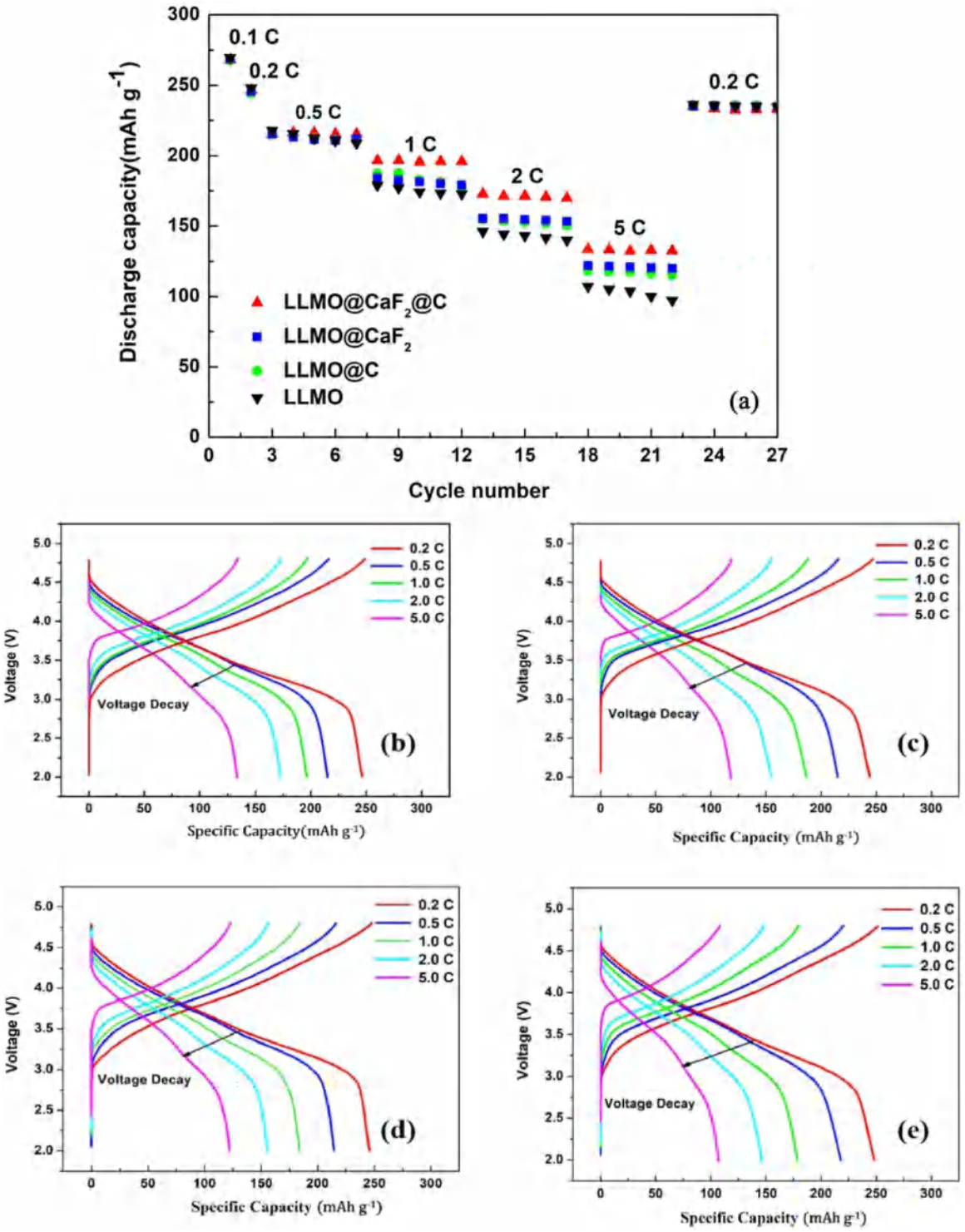


**Fig. 6.** (a) the rate performance curves of all samples, (b-e) the charge and discharge curves of all samples at 0.2 C, 0.5 C, 1 C, 2 C, 5 C, (f-i) dQ/dV plots of all samples at 0.2 C, 0.5 C, 1 C, 2 C, 5 C.,.

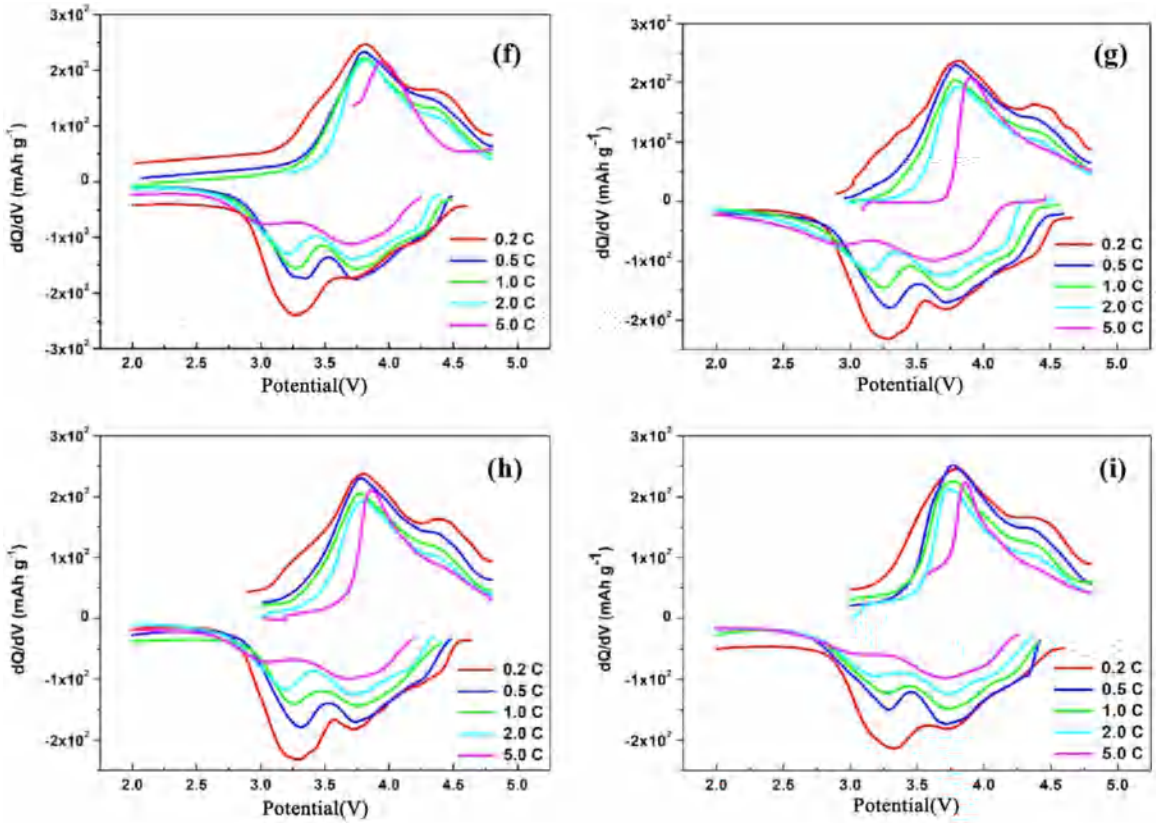


**Fig. 6.** (*continued*)

better cycle performance than LLMO-II, LLMO-III, LLMO-IV. In details, the discharge specific capacity of LLMO -I reaches 215.2 mA h g-1 at the 0.5 C and 195.4 mA h $g^{-1}$ after 150 cycles. While LLMO-II, LLMO-III, LLMO-IV are only 165.6 mA h $g^{-1}$, 151.2 mA h $g^{-1}$ and 137.2 mA h $g^{-1}$ after 150 cycles respectively. In order to further observe the charge/discharge curve changes during the cycle, the charge/discharge curves of all samples, which were cycled for 1 time, 30 times, 60 times, 90 times,120 times, 150 times, are plotted. As shown in Fig. 5c-f, it can be easily observed that all samples display the different levels of voltage decay. What's notable in Fig. 5c-f is that voltage decay of LLMO -I is the least. The reason why LLMO-I has the best excellent cycling performance in all samples can attributed to two aspects: Firstly, $CaF_2$ and Graphite, acting as two-layer coatings, not only protect the active material from the erosion of electrolytes, but also avoid the occurrence of microcracks in inner material caused by charging and discharging stress. Secondly, the transition layer, which contain $Li_{1.2}Mn_{0.54}Ni_{0.13}Co_{0.13}O_2$, $Ca^{2+}$, $F^-$, can inhibit the deinsertion of O-ion from the lattice and restrain the surface phase transition of Lithium-rich layered oxide material.

Improving the rate performance of Lithium-rich layered oxide material is another challenge for researcher. In order to observe whether $CaF_2$ and Graphite two-layer coating effects the rate performance of Lithium-rich layered oxide material, the curves of all samples at 0.2 C, 0.5 C, 1 C, 2 C, 5 C are plotted and the detail discharge data at different rate are summarized in Table 2. As shown in Fig. 6a, it is obvious observed that LLMO-I displays the best rate performance. In order to further observe the charge/discharge curve changes when the charge/discharge current vary, the charge and discharge curves of all samples at 0.2 C, 0.5 C, 1 C, 2 C, 5 C are plotted. It can be seen in Fig. 6b-e that all samples exhibit voltage decay when the charge/discharge current increases. Note that LLMO-I has the least voltage decay. In order to further analyze the reason why lithium-rich layered oxide material exhibits voltage decay along with the rate increase, dQ/dV plots of all samples at 0.2 C, 0.5 C, 1 C, 2 C, 5 C are calculated. As present in Fig. 6f-i, with the increase of rate, the redox strength of $Mn^{4+}/Mn^{3+}$ gets weak, and the redox strength of $Ni^{4+}/Ni^{2+}$ and $Co^{4+}/Co^{3+}$ get intense. This phenomenon implies that the reason why Li-rich layered oxide material exhibits the poor rate performance mainly attribute to the weak electrochemical activity of $LiMn_2O_3$. Besides, it also can be found in Fig. 6f-i that LLMO-I exhibits the least voltage decay and stronger redox strength of $Mn^{4+}/Mn^{3+}$. The reasons why LLMO -I displays the best rate performance mainly contain follow aspect: one hand, $CaF_2$ and Graphite two-layer coatings can protect active material from the erosion of electrolyte and inhibit the dissolution of $Mn^{4+}$ from the oxide into electrolyte. On the other hand, Graphite has a better electronic conductivity, which can decrease the interfacial resistance of lithium insertion/extraction.

To understand the impact of $CaF_2$ and Graphite two-layer coatings on the electrode resistance, the EIS of all samples were conducted [32,33]. As presented in Fig. 7a and b, it could be obvious observed that LLMO-I and LLMO-II have a smaller $R_{SEI}$ (the resistance the lithium-ion through the SEI films) than LLMO-III and LLMO-IV, which indicate $CaF_2$ coating can induce the formation of excellent SEI film. Besides, the LLMO-I has the least Rct (the charge transfer resistance) in all samples, which further implies $CaF_2$ and Graphite two-layer coatings can decrease the electrode resistance of lithium-rich layered oxide material. The reason why LLMO-I presents the best performance of electrode resistance can own two aspect. One side, $CaF_2$ has the fluorite structure, which can offer lots of diffusion paths for lithium-ion migration. For another, Graphite is an excellent electronic conductor and can increase the electronic conductivity of inner active material.

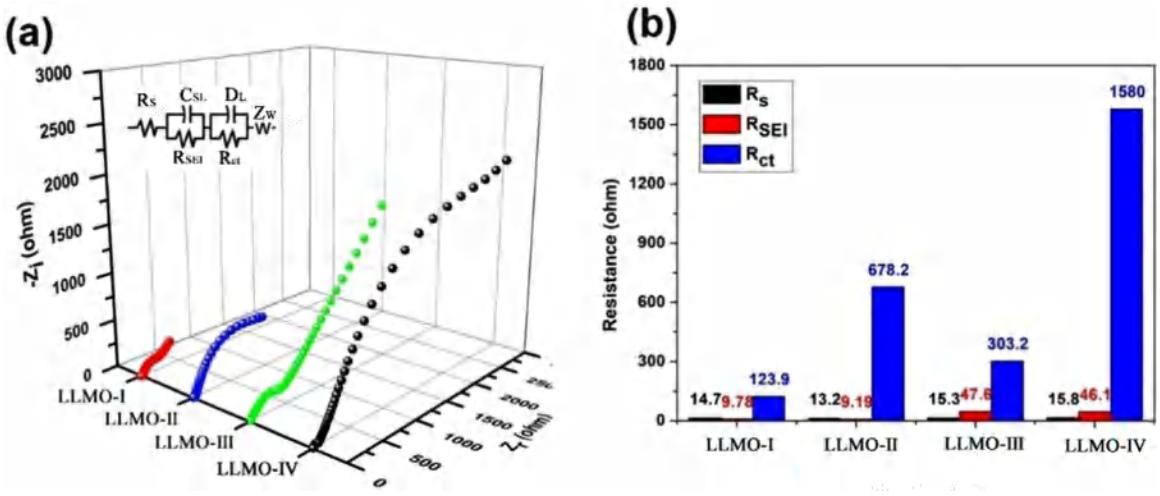


**Fig. 7.** (a)Electrochemical impedance spectras of) LLMO-I, LLMO-II, LLMO-III, LLMO-IV, and the inserted equivalent circuit is used for data fitting and (b) corresponding fitted parameters of all fresh cells.

## 4. Conclusion

In summary, the combined effect of $CaF_2$ and Graphite two-layer coatings are studied to further prompt the commercialization of Lithium-rich layered oxide materials in this work. The results of EDS and TEM show $CaF_2$ and Graphite have been wrapped on the surface of Lithium-rich layered oxide material. Based on the electrochemical characterization and evaluation, LLMO-I exhibits the best electrochemical performance, which can attribute to the $CaF_2$ and Graphite two-layer coatings. $CaF_2$, acting as the inner coating layer, has excellent Lithium-ion migration velocity and good stability in acidic electrolytes. Graphite, acting as the outer coating layer, can decrease the interfacial resistance for lithium insertion/extraction and enhance the stability of inner material. The two-layer coatings of $CaF_2$ and Graphite, which can take advantage of the $CaF_2$ demo-coating and Graphite demo-coating, would be a promising method and could further prompt the commercialization of Lithium-rich layered oxide materials.

## Acknowledgements

The Shanghai Scientific and Technological Innovation Project(18JC1410600), Research and Development of High Voltage Electrolyte for Lithium Ion Power Battery Based on Fluorine Solvent System (18511110000), The National Program on Key Basic Research Project (No. 2015CB931900).

## References

[1] F. Wu, N. Li, Y. Su, L. Zhang, L. Bao, J. Wang, et al., Ultrathin spinel membrane-encapsulated layered lithium-rich cathode material for advanced Li-ion batteries, Nano Lett. 14 (2014) 3550–3555.
[2] W. Wei, L. Chen, A. Pan, D.G. Ivey, Roles of surface structure and chemistry on electrochemical processes in lithium-rich layered oxide cathodes, Nano Energy 30 (2016) 580–602.
[3] Y. Zhu, X. Luo, M. Xu, L. Zhang, L. Yu, W. Fan, et al., Failure mechanism of layered lithium-rich oxide/graphite cell and its solution by using electrolyte additive, J. Power Sources 317 (2016) 65–73.
[4] L. Riekehr, J. Liu, B. Schwarz, F. Sigel, I. Kerkamm, Y. Xia, et al., Fatigue in 0.5Li2MnO3:0.5Li(Ni1/3Co1/3Mn1/3)O2 positive electrodes for lithium ion batteries, J. Power Sources 325 (2016) 391–403.
[5] S. Chong, Y. Chen, W. Yan, S. Guo, Q. Tan, Y. Wu, et al., Suppressing capacity fading and voltage decay of Li-rich layered cathode material by a surface nano-protective layer of CoF 2 for lithium-ion batteries, J. Power Sources 332 (2016) 230–239.
[6] D. Qian, B. Xu, M. Chi, Y.S. Meng, Uncovering the roles of oxygen vacancies in cation migration in lithium excess layered oxides, Phys. Chem. Chem. Phys. 16 (2014) 14665–14668.
[7] K. Luo, M.R. Roberts, R. Hao, N. Guerrini, E. Liberti, C.S. Allen, et al., One-pot synthesis of lithium-rich cathode material with hierarchical morphology, Nano Lett. 16 (2016) 7503–7508.
[8] Y. Wu, A. Vadivel Murugan, A. Manthiram, Surface modification of high capacity layered Li[Li[sub 0.2]Mn[sub 0.54]Ni[sub 0.13]Co[sub 0.13]]O[sub 2] cathodes by AlPO[sub 4], J. Electrochem. Soc. 155 (2008) A635.
[9] S. Shi, S. Zhang, Z. Wu, T. Wang, J. Zong, M. Zhao, et al., Full microwave synthesis of advanced Li-rich manganese based cathode material for lithium ion batteries, J. Power Sources 337 (2017) 82–91.
[10] Q. Li, G. Li, C. Fu, D. Luo, J. Fan, L. Li, K(+)-doped Li(1.2)Mn(0.54)Co(0.13)Ni(0.13)O2: a novel cathode material with an enhanced cycling stability for lithium-ion batteries, ACS Appl. Mater. Interfaces 6 (2014) 10330–10341.
[11] H. Yu, R. Ishikawa, Y.G. So, N. Shibata, T. Kudo, H. Zhou, et al., Direct atomic-resolution observation of two phases in the Li(1.2)Mn(0.567)Ni(0.166)Co(0.067)O2 cathode material for lithium-ion batteries, Angew. Chem. 52 (2013) 5969–5973.
[12] Y. Wang, Z. Yang, Y. Qian, L. Gu, H. Zhou, New insights into improving rate performance of lithium-rich cathode material, Adv. Mater. 27 (2015) 3915–3920.
[13] L. Chen, Y. Su, S. Chen, N. Li, L. Bao, W. Li, et al., Hierarchical Li1.2 Ni0.2 Mn0.6 O2 nanoplates with exposed {010} planes as high-performance cathode material for lithium-ion batteries, Adv. Mater. 26 (2014) 6756–6760.
[14] Y.X. Wang, K.H. Shang, W. He, X.P. Ai, Y.L. Cao, H.X. Yang, Magnesium-doped Li1.2[Co0.13Ni0.13Mn0.54]O2 for lithium-ion battery cathode with enhanced cycling stability and rate capability, ACS Appl. Mater. Interfaces 7 (2015) 13014–13021.
[15] X. Liu, J. Liu, T. Huang, A. Yu, CaF2-coated Li1.2Mn0.54Ni0.13Co0.13O2 as cathode materials for Li-ion batteries, Electrochim. Acta 109 (2013) 52–58.
[16] D. Chen, W. Tu, M. Chen, P. Hong, X. Zhong, Y. Zhu, et al., Synthesis and performances of Li-Rich@AlF 3 @Graphene as cathode of lithium ion battery, Electrochim. Acta 193 (2016) 45–53.
[17] Y.K. Sun, M.J. Lee, C.S. Yoon, J. Hassoun, K. Amine, B. Scrosati, The role of AlF3 coatings in improving electrochemical cycling of Li-enriched nickel-manganese oxide electrodes for Li-ion batteries, Adv. Mater. 24 (2012) 1192–1196.
[18] J. Zhang, Q. Lu, J. Fang, J. Wang, J. Yang, Y. NuLi, Polyimide encapsulated lithium-rich cathode material for high voltage lithium-ion battery, ACS Appl. Mater. Interfaces 6 (2014) 17965–17973.
[19] L. Guo, N. Zhao, J. Li, C. He, C. Shi, E. Liu, Surface double phase network modified lithium rich layered oxides with improved rate capability for Li-ion batteries, ACS Appl. Mater. Interfaces 7 (2015) 391–399.
[20] H. Konishi, T. Hirano, D. Takamatsu, A. Gunji, X. Feng, S. Furutsuki, Evaluation of stability of charged lithium-rich layer-structured cathode material at elevated temperature, Electrochim. Acta 169 (2015) 310–316.
[21] M. Li, Y. Zhou, X. Wu, L. Duan, C. Zhang, F. Zhang, et al., The combined effect of CaF 2 coating and La-doping on electrochemical performance of layered lithium-rich cathode material, Electrochim. Acta 275 (2018) 18–24.
[22] C. Chen, T. Geng, C. Du, P. Zuo, X. Cheng, Y. Ma, et al., Oxygen vacancies in SnO2 surface coating to enhance the activation of layered Li-Rich Li1.2Mn0.54Ni0.13Co0.13O2 cathode material for Li-ion batteries, J. Power Sources 331 (2016) 91–99.
[23] R. Yu, G. Wang, M. Liu, X. Zhang, X. Wang, H. Shu, et al., Mitigating voltage and capacity fading of lithium-rich layered cathodes by lanthanum doping, J. Power Sources 335 (2016) 65–75.
[24] A. Boulineau, L. Simonin, J.F. Colin, C. Bourbon, S. Patoux, First evidence of manganese-nickel segregation and densification upon cycling in Li-rich layered oxides for lithium batteries, Nano Lett. 13 (2013) 3857–3863.
[25] Y. Zhou, P. Bai, H. Tang, J. Zhu, Z. Tang, Chemical deposition synthesis of desirable high-rate capability Al 2 O 3 -coated Li 1.2 Mn 0.54 Ni 0.13 Co 0.13O2 as a Lithium ion battery cathode material, J. Electroanal. Chem. 782 (2016) 256–263.
[26] L. He, J. Xu, T. Han, H. Han, Y. Wang, J. Yang, et al., SmPO4-coated Li1.2Mn0.54Ni0.13Co0.13O2 as a cathode material with enhanced cycling stability for lithium ion batteries, Ceram. Int. 43 (2017) 5267–5273.
[27] J. Li, T. Jia, K. Liu, J. Zhao, J. Chen, C. Cao, Facile design and synthesis of Li-rich nanoplates cathodes with habit-tuned crystal for lithium ion batteries, J. Power Sources 333 (2016) 37–42.
[28] R.-P. Qing, J.-L. Shi, D.-D. Xiao, X.-D. Zhang, Y.-X. Yin, Y.-B. Zhai, et al., Enhancing the kinetics of Li-rich cathode materials through the pinning effects of

gradient surface Na+ doping, Adv. Energy Mater. 6 (2016) 1501914.
[29] X. Jin, Q. Xu, X. Liu, X. Yuan, H. Liu, Improvement in rate capability of lithium-rich cathode material Li[Li0.2Ni0.13Co0.13Mn0.54]O2 by Mo substitution, Ionics 22 (2016) 1369–1376.
[30] Q.-Q. Qiao, G.-R. Li, Y.-L. Wang, X.-P. Gao, To enhance the capacity of Li-rich layered oxides by surface modification with metal–organic frameworks (MOFs) as cathodes for advanced lithium-ion batteries, J. Mater. Chem. A 4 (2016) 4440–4447.
[31] B. Qiu, M. Zhang, L. Wu, J. Wang, Y. Xia, D. Qian, et al., Gas-solid interfacial modification of oxygen activity in layered oxide cathodes for lithium-ion batteries, Nat. Commun. 7 (2016) 12108.
[32] Z. Wang, E. Liu, L. Guo, C. Shi, C. He, J. Li, et al., Cycle performance improvement of Li-rich layered cathode material Li[Li0.2Mn0.54Ni0.13Co0.13]O2 by ZrO2 coating, Surf. Coat. Technol. 235 (2013) 570–576.
[33] Y. Li, C. Wu, Y. Bai, L. Liu, H. Wang, F. Wu, et al., Hierarchical mesoporous lithium-rich Li[Li0.2Ni0.2Mn0.6]O2 cathode material synthesized via ice templating for lithium-ion battery, ACS Appl. Mater. Interfaces 8 (2016) 18832–18840.